Indonesian Journal of Electrical Engineering and Informatics (IJEEI)
Vol. 10, No. 4, December 2022, pp. 796~803
ISSN: 2089-3272, DOI: 10.52549/ijeei.v10i4.4032

Restoration of Blurred and Noisy Images Using Inverse Filtering and Adaptive Threshold Method

Zayed M. Ramadan
Department of Electrical Engineering, College of Engineering, King Faisal University, Saudi Arabia

Article Info

Article history:

Received Jun 29, 2022
Revised Nov 11, 2022
Accepted Nov 27, 2022

Keywords:

Blur
Impulse Noise
Inverse Filtering
Image Filtering
Image Restoration

ABSTRACT

A restoration scheme for images that are corrupted with both blur and impulsive noise is proposed in this paper to reconstruct an image with minimum degradation. The restoration scheme consists of two stages in sequence where the first stage is applied to the blurred image and the second stage is applied to de-blurred image that has been subject to noise through electronic transmission. The first stage uses frequency domain filtering while the second utilizes spatial filtering to reduce the indicated blur and noise, respectively. In particular, truncated inverse filtering is used for reducing the blur and an adaptive algorithm with an estimated threshold is used for minimizing the noise. Simulation of the introduced method uses several performance measuring indices such as mean absolute error (MAE) and peak signal-to-noise ratio (PSNR). Results of these simulations show great performance of the proposed method in terms of reducing the blur and noise significantly while keeping details and sharpness of the image edges.

Corresponding Author:

Zayed M. Ramadan,
Department of Electrical Engineering, College of Engineering,
King Faisal University,
Al Hofuf 31982, Saudi Arabia
Email: zramadan@kfu.edu.sa

1. INTRODUCTION

Image restoration is one of the main areas of image processing that deals with the elimination or reduction of degradation that images have been subject to [1-3]. Image degradation is often known or estimated and the aim of image restoration then is to reconstruct the original image appearance. If a model for the degradation process is available, the inverse process or inverse filtering can be applied to restore the image to its original form.

The image degradations may include blurring due to camera motion, for example, [4-18] or noise which is effectively equivalent to errors in the image pixel values and is due to many causes such as electronic image transmission [19-27]. Law enforcement, for example, is an application of image restoration in which the image is blurred due to motion. In several situations, it might be necessary to read the letters on a blurred item on a moving object such as a blurred license plate on a moving car or even identifying a human face in the car.

Many authors in the field of image processing have been working on developing algorithms or schemes to improve the quality of images that are subject to blur and noise. In [4], some restoration methods such as inverse filter, Weiner filter and Last Squares (LS) are implemented and analyzed. An image restoration with estimation of the point spread function (PSF) and using Weiner filtering and inverse filtering for images blurred by motion is presented in [5]. In [6], a blind deconvolution method is proposed to restore ultrasound images based on inverse filtering with a restoration kernel. A method is proposed in [7] to estimate the optimum level of noise elimination of the two-dimensional inverse filter. A comparison between inverse filter and Wiener filter in reducing noise and blur is shown in [8]. In [9], a two-stage parametric inverse filtering scheme is proposed for restoration of ultrasound images. The introduced algorithm in [10] uses sparse representation of double discrete wavelet transform to reconstruct low light photos that are contaminated with noise and blur. Invariants to Gaussian blur proposed in [11] can find applications in blur-invariant image recognition.

The proposed scheme in [12] uses a blur kernel that consists of a linear combination of basic two dimensional (2-D) patterns. The introduced method in [13] removes the motion blur based on transformation of the 2-D blurred image into one dimensional (1-D) horizontal blurred vectors. In [14], adaptive optics images are restored using maximum a posteriori estimation with image Gaussian statistics and blur kernel. The proposed scheme in [15] addresses the problem of blind image deconvolution using multiple blurry images algorithm. In [16], the proposed image deblurring method increases the frequency fall-off of the PSF by convolving the blurry input images with a deconvolution kernel composed of a linear combination of finite impulse response (FIR) filters. Estimation of blur kernels is not required in the introduced scheme in [17] using two images acquired in low light. In [18], the proposed method classifies the image blur into intentional blur and unintentional blur.

In [19, 21, 22, 24, 25, 27] several methods are proposed to reduce the impulse noise utilizing spatial domain. The proposed methods in [20, 23, 26] employ non-local mean (NLM) methods for image restoration. In this paper, the first stage of the proposed image restoration scheme reduces blur using inverse truncated filtering algorithm. In the second stage, the proposed scheme minimizes the impulse noise using a spatial-domain method using a slide filtering window of an adaptive size varying based on the estimated impulsive noise percentage.

2. PROPOSED METHOD

The PSF of the imaging system as it is often called in image processing is equivalent to the well-known function called impulse response of the system, which is the output or the response of the system when the input is a Dirac delta function. Similarly, the PSF measures the spread in the imaging system output intensity due to an infinitely sharp input point. The PSF is of a crucial importance because it completely characterizes the imaging system in the sense that given the PSF of the system, the output of the system can be determined for any given input using convolution.

The Optical Transfer Function (OTF) denoted by $H(n_x, n_y)$ of an imaging system is the Fourier transform of the PSF. The Modulation Transfer Function (MTF) denoted by $M(n_x, n_y)$ is the magnitude square of the OTF and is defined by

$$M(n_x, n_y) = |H(n_x, n_y)| \quad (1)$$

Since the OTF is in general complex-valued, the MTF is a real-valued function.

The inverse filter denoted by $I(n_x, n_y)$ can be defined as

$$I(n_x, n_y) = \frac{1}{H(n_x, n_y)} \quad (2)$$

Evidently, the recovery of any input spatial frequency (n_x, n_y) at which the value of $H(n_x, n_y)$ is close to zero results in an infinite value of $I(n_x, n_y)$ which is reflected in calamitous results. To solve this problem, a truncated inverse filter is used in this paper where $I(n_x, n_y)$ is set to zero whenever $H(n_x, n_y)$ is below a small predetermined threshold value. The steps of the inverse filtering are as follows:

Construct Gaussian PSF and extend it over the entire matrix that represents the image.
Find $H(n_x, n_y)$ that corresponds to the PSF.
Generate blurred image via Fourier transform (FT).
Find the FT of the image.
Perform truncated inverse filtering.

In the second stage of the proposed method, impulsive noise and in particular salt-and-pepper noise is used in the simulation results. The noisy pixels are determined based on whether the pixel values are either minimum value (0) or maximum value (255). The uncorrupted pixels are untouched and only the noisy pixels are processed by replacing each corrupted pixel value by the average value of the remaining pixel values in the

filtering window [19]. The noise percentage or density *ND* is the ratio of the estimated number of noisy pixels to the total number of pixels in the image, and is defined as follows:

$$ND = N_i / K.L, \tag{3}$$

where N_i is the estimated number of noisy pixels and the product $K.L$ is the total number of noisy pixels in the processed image [19].

The filtering window in the adaptive threshold method is the small sliding window on which the filtering process is being applied. The common values of the size of this filtering window $S \times S$ are 3×3, 5×5 or 7×7 depending on the noise density *ND*. The larger the noise density is, the larger the size of the window [24, 26].

$$S \times S = \begin{cases} 3 \times 3 & ND \leq 45\% \\ 5 \times 5 & 45\% \leq ND \leq 75\% \\ 7 \times 7 & ND \geq 75\% \end{cases} \tag{4}$$

The largest size of the filtering window used in this paper is $S \times S = 7 \times 7$ for a noise density $ND = 90\%$ which is an extremely high value.

Various measuring quality metrics indices are typically used in the field of image restoration to measure the quality of the filtering methods or schemes [2], i.e., the similarity or closeness between the original clean image and the recovered image. In addition, those indices measure the capabilities of the filtering schemes to preserve the sharp edges and fine details in the tested images.

In this paper, Mean Absolute Error (MAE) and Peak Signal to Noise Ratio (PSNR) in decibels (dB) are used to measure the performance of the proposed method. The MAE measures the average of the absolute error pixel values between the original and filtered images. The PSNR can be expressed as a function of the mean square error (MSE). The MSE is an average of the total summation of the square errors between the input and output pixels of the image filtering scheme. The lower the value of MSE or MAE, the lower the error and the higher the similarity between the original clean image and the restored image. In contrast, the higher the value of PSNR, the lower the error and the higher the closeness between the clean image and the filtered one.

These performance measuring indices are defined as follows:

$$MAE = \frac{1}{KL} \sum_{i=1}^{K} \sum_{j=1}^{L} \left| F_{i,j} - C_{i,j} \right| \tag{5}$$

$$PSNR = 10\, log_{10} \left(\frac{(N-1)^2}{MSE} \right) \text{ dB}, \tag{6}$$

where MSE is defined by

$$MSE = \frac{1}{KL} \sum_{i=1}^{K} \sum_{j=1}^{L} \left(F_{i,j} - C_{i,j} \right)^2 \tag{7}$$

The MAE is the mean absolute error between the recovered filtered output image (*F*) and the clean uncorrupted input image (*C*), $N = 2^n$ where n is the number of bits used to represent each pixel (also called the bit depth of an image), *K* is the number of pixels in the horizontal dimension of the image which is equivalent to the number of rows in the matrix that represents the image, and *L* is number of pixels in the vertical dimension of the image which is equivalent to the number of columns in the matrix that represents that image. Finally, $F_{i,j}$ and $C_{i,j}$ are the pixel values in the $(i,j)th$ locations of the output filtered image and the original clean input image, respectively.

For a grayscale image with a bit depth of 8 bits per pixel, for example, there will be $(2^8 - 1)^2 = 255^2 = 65025$ as the numerator of the PSNR.

3. RESULTS AND DISCUSSION

Many images have been tested using the proposed method. However, the results of using three images are shown in this section of the paper, namely Lake, Lina and Cameraman images. Figures 1, 2 and 3 show simulation results of the proposed method using Lake image with low, medium and high amount of blur, respectively, and impulse noise percentage of 50%. Figures 1.a, 2.a, 3.a depicts the PSF and MTF in each of the three cases mentioned above. As clearly demonstrated from these figures, the larger the circle at the center of the MTF, the less blurred the image, and the smaller the circle, the more blurred the image is.

It should be noted that in practice, the system PSF could be random or deterministic. Typically, it is a deterministic quantity that is entirely dependent on the physical nature of the image processing system hardware. Once the imaging system design is completed, the system PSF is considered as a fixed quantity. On the other hand, noise is typically random and is usually modeled using statistical measurements.

In addition, it is of a crucial importance to emphasize that a truncated inverse filter has been used in the simulations in this paper. In such a filter, an infinity value of the inverse filter $I(n_x, n_y)$, and hence an unstable system, is avoided by setting its value to zero whenever $H(n_x, n_y)$ approaches a predetermined low threshold value. In the simulation results in this paper, the threshold value used is 1×10^{-6}.

Figures 1.b, 2.b, 3.b illustrate the performance of the inverse filtering in the first stage of the proposedistic function method. In each of these three figures, the original clean Lake image, the blurred image and the recovered (de-blurred) image are shown. The recovered image is very similar to the original clean image as depicted in these figures.

Figures 1.c, 2.c, 3.c show the performance of the overall proposed filtering scheme. The restored image in the inverse filtering stage is subjected to impulse noise of 50% and this noisy image is processed in the second stage of the proposed method to produce the final reconstructed image. From both quantitative and qualitative results, the introduced method shows superior performance in reducing the blur and noise and preserving the details and sharpness of the image.

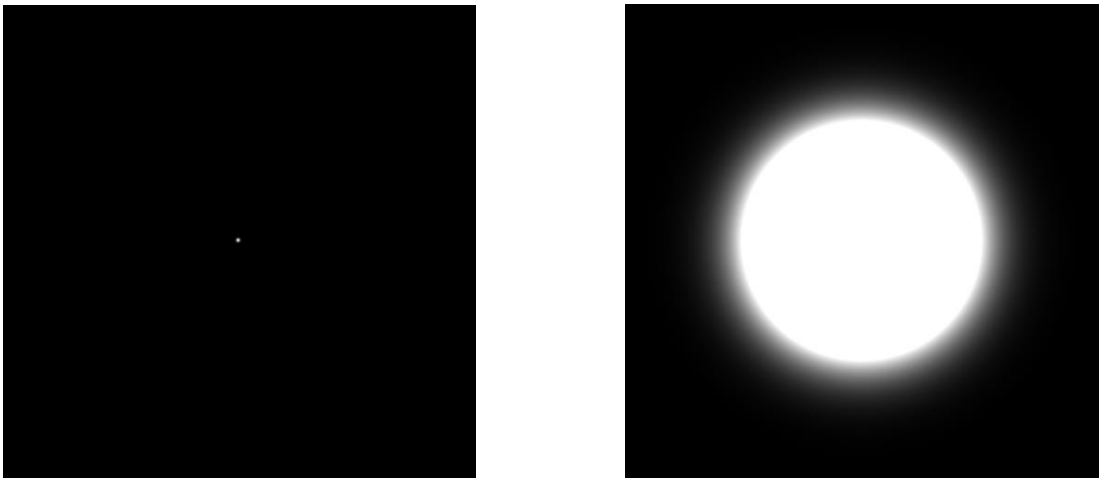

Figure 1. a. PSF and MTF for a small amount of blur in the inverse filtering stage of the proposed method

Figure 1. b. Lake image: before being blurred by a small amount of blur, after being blurred and the deblurred image using inverse filtering

Figure 1. c. Deblurred Lake image: before being corrupted by noise with ND =50% of impulse noise, after being noised and the restored image using the second stage of the proposed method.

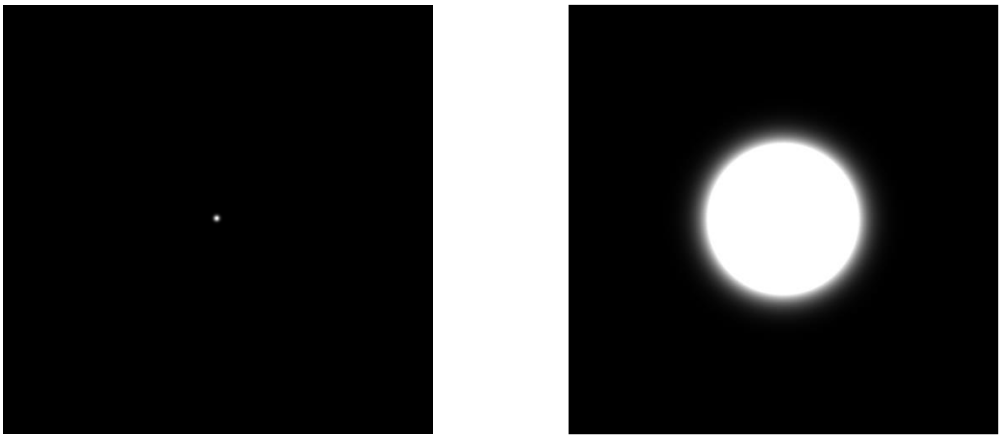

Figure 2. a. PSF and MTF for a medium quantity of blur in the inverse filtering stage of the proposed method

Figure 2. b. Lake image: before being blurred by a medium amount of blur, after being blurred and the deblurred image using inverse filtering

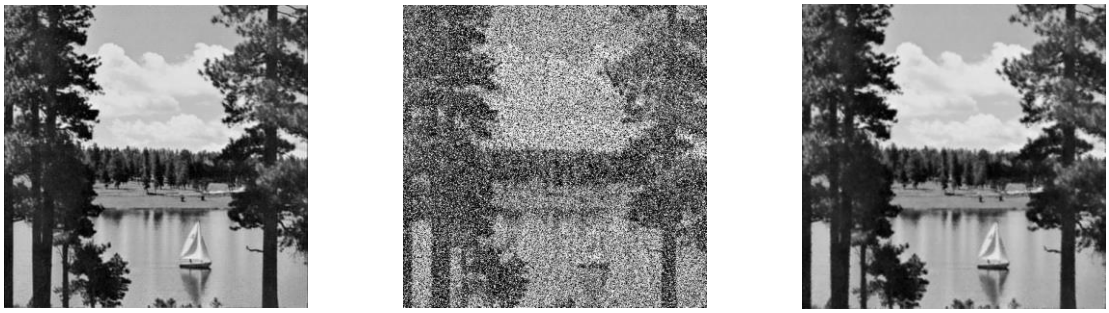

Figure 2. c. Deblurred Lake image: before being corrupted by noise with ND =50% of impulse noise, after being noised and the restored image using the second stage of the proposed method.

Figure 3. a. PSF and MTF for a more quantity of blur in the inverse filtering stage of the proposed method

Figure 3. b. Lake image: before being blurred by a high amount of blur, after being blurred and the restored image using inverse filtering

Figure 3. c. Deblurred Lake image: before being corrupted by noise with ND =50% of impulse noise, after being noised and the restored image using the second stage of the proposed method.

Large number of images have been examined through simulations using the proposed method. However, some images of different characteristics, edge details and sharpness have been selected in this paper. In addition, images corrupted with wide ranges of blur and noise quantities have been used and the corresponding simulation results are shown and analyzed in this paper.

Simulation results of the proposed method using three images, namely Lake, Lina and Cameraman are shown in Table 1, Table 2 and Table 3, respectively. In these three tables, MAE and PSNR are listed for three impulse noise densities: 10%, 50% and 90% and for three levels of blur: low, medium and high. Improvements in PSNR values (high values) and in MAE (low values) are clearly illustrated in these tables for the indicated wide range of noise and blur amounts.

The MAE0 and PSNR0 metrics are computed by Equations (5-7) using the original and the corrupted images while MAE1 and PSNR1 are computed by the same equations using the original and the restored images produced by the proposed method.

Table 1. MAE and PSNR in the proposed method using the Lake image before and after corrupted by various amounts of blur and impulse noise.

Proposed Method ($ND = 10\%$)	**MAE0**	**MAE1**	**PSNR0 (dB)**	**PSNR1 (dB)**
Small Blur	19.92	7.93	14.76	27.56
Medium Blur	22.36	10.70	14.66	25.47
High Blur	28.00	16.96	14.30	22.09
Proposed Method ($ND = 50\%$)				
Small Blur	67.61	9.00	8.00	25.94
Medium Blur	69.23	11.51	7.97	24.45
High Blur	72.43	17.36	7.91	21.73
Proposed Method ($ND = 90\%$)				
Small Blur	115.88	13.38	5.44	21.66
Medium Blur	115.78	15.20	5.45	21.08
High Blur	116.41	20.14	5.45	19.64

Table 2. MAE and PSNR in the proposed method using the Lina image before and after corrupted by various amounts of blur and impulse noise.

Proposed Method ($ND = 10\%$)	**MAE0**	**MAE1**	**PSNR0 (dB)**	**PSNR1 (dB)**
Small Blur	29.11	18.31	14.58	21.27
Medium Blur	32.96	22.31	14.15	19.77
High Blur	37.11	26.91	13.76	18.36
Proposed Method ($ND = 50\%$)				
Small Blur	72.91	18.55	8.34	21.01
Medium Blur	75.01	22.53	8.29	19.59
High Blur	77.04	26.98	8.26	18.29
Proposed Method ($ND = 90\%$)				
Small Blur	116.52	21.14	5.90	19.33
Medium Blur	116.74	24.64	5.90	18.41
High Blur	117.27	28.48	5.89	17.56

Table 3. MAE and PSNR in the proposed method of the Cameraman image before and after corrupted by to various amounts of blur and impulse noise.

Proposed Method ($ND = 10\%$)	**MAE0**	**MAE1**	**PSNR0 (dB)**	**PSNR1 (dB)**
Small Blur	23.65	12.17	14.78	25.82
Medium Blur	23.57	11.98	14.75	25.98
High Blur	25.49	14.22	14.68	24.43
Proposed Method ($ND = 50\%$)				
Small Blur	70.12	12.88	8.03	24.81
Medium Blur	69.70	12.65	8.06	24.97
High Blur	71.03	14.77	8.03	23.77
Proposed Method ($ND = 90\%$)				
Small Blur	116.21	15.72	5.52	21.74
Medium Blur	115.94	15.53	5.53	21.83
High Blur	116.36	17.41	5.52	21.21

In these tables, an adaptive size of the kernel filter has been utilized in the second stage of the proposed filtering scheme based on the estimated number of pixels that have been corrupted by noise. The size of the filter increases as the noise percentage increases and vice versa. The difference in the results of these three tables tables are due to the differences between the characteristias, details, edges and sharpness of these three tested images. While the PSNR metric is a function of the MSE which squares the pixel differences between two images, the MAE does not square or weight the absolute values of these differences, and thus it increases linearly as the absolute error increases and vice versa.

4. CONCLUSION

A restoration filtering scheme for blurry and impulsive noisy images has been proposed in this paper. The first stage of the method uses inverse filtering for recovery of the blurred image assuming that the blurring function is known. The recovered image of the first stage is subject to impulse noise through electronic transmission and is processed in the second stage of the introduced filtering method to reduce this noise. The MAE and PSNR are used to measure the image quality of the method. Superior results have been obtained using many tested gray-scale images of different characteristics and subjected to a broad range of noise density values and blur amounts.

REFERENCES

[1] Aymeric Histace. Image Restoration – Recent Advances and Applications. InTech, 2012.
[2] Chi-Wah Kok and Wing-Shan Tam. Digital Image Interpolation in MATLAB. John Wiley & Sons Singapore, 2019.

[3] Scott E Umbaugh. Digital Image Processing and Analysis: Applications with MATLAB and CVIPtools. CRC Press, 2018.
[4] R. P. Kumar, S. C. Neela, S. Reddy Murikinati, M. Reddy Yachavarapu and A. Reddy Gayam. Image Restoration by Inverse Filtering. Sixth International Conference on Computing Methodologies and Communication (ICCMC). 2022; 1227-1231.
[5] S. Jia and J. Wen. Motion blurred image restoration. Sixth International Congress on Image and Signal Processing (CISP). 2013; 384-389.
[6] O. Michailovich and A. Tannenbaum. Deconvolution of medical ultrasound images via parametric inverse filtering. 3rd IEEE International Symposium on Biomedical Imaging: Nano to Macro. 2006; 217-220.
[7] T. Daboczi and T. B. Bako. Inverse filtering of optical images. IEEE Transactions on Instrumentation and Measurement. 2001; 50(4): 991-994.
[8] M. M. R. Khan, S. Sakib, R. B. Arif and M. A. B. Siddique. Digital Image Restoration in Matlab: A Case Study on Inverse and Wiener Filtering. International Conference on Innovation in Engineering and Technology (ICIET). 2018; 1-6.
[9] O. Michailovich and A. Tannenbaum. Blind Deconvolution of Medical Ultrasound Images: A Parametric Inverse Filtering Approach. IEEE Transactions on Image Processing. 2007; 16(12): 3005-3019.
[10] Y. Zhang and K. Hirakawa. Blind Deblurring and Denoising of Images Corrupted by Unidirectional Object Motion Blur and Sensor Noise. IEEE Transactions on Image Processing. 2016; 25(9): 4129-4144.
[11] J. Flusser, S. Farokhi, C. Höschl, T. Suk, B. Zitová and M. Pedone. Recognition of Images Degraded by Gaussian Blur. Transactions on Image Processing. 2016; 25(2):790-806.
[12] C. Lee and W. Hwang. Mixture of Gaussian Blur Kernel Representation for Blind Image Restoration. IEEE Transactions on Computational Imaging. 2017; 3(4): 783-797.
[13] H. Hong and Y. Shi. Fast Deconvolution for Motion Blur Along the Blurring Paths. Canadian Journal of Electrical and Computer Engineering. 2017; 40(4): 266-274.
[14] D. Li, G. Qiu and L. Zhang. Adaptive Optics Image Restoration via Regularization Priors with Gaussian Statistics. IEEE Access. 2020; 8: 3364-3373.
[15] T. -C. Lin, L. Hou, H. Liu, Y. Li and T. -K. Truong. Reconstruction of Single Image from Multiple Blurry Measured Images. IEEE Transactions on Image Processing. 2018; 27(6): 2762-2776.
[16] M. S. Hosseini and K. N. Plataniotis. Convolutional Deblurring for Natural Imaging. IEEE Transactions on Image Processing. 2020; 29: 250-264.
[17] C. Gu, X. Lu, Y. He and C. Zhang. Blur Removal Via Blurred-Noisy Image Pair. IEEE Transactions on Image Processing. 2021; 30: 345-359.
[18] R. Huang, M. Fan, Y. Xing and Y. Zou. Image Blur Classification and Unintentional Blur Removal. IEEE Access. 2019; 7: 106327-106335.
[19] Ramadan ZM. Monochromatic-Based Method for Impulse Noise Detection and Suppression in Color Images. Circuits, Systems, and Signal Processing. 2013; 32(4): 1859-1874.
[20] Zayed M. Ramadan. An Innovative Kernel Function for the NLM Filtering, ARPN Journal of Engineering and Applied Sciences. 2020; 15(7): 882-889.
[21] Veerakumar T, Jagannath, RP, Subudhi BN, Esakkirajan S. Impulse Noise Removal Using Adaptive Radial Basis Function Interpolation. Circuits, Systems, and Signal Processing. 2017; 36(3): 1192-1223.
[22] Ramadan ZM. A New Method for Impulse Noise Elimination and Edge Preservation. Canadian Journal of Electrical and Computer Engineering. 2014; 37(1): 2-10.
[23] D. Zeng et al. Spectral CT Image Restoration via an Average Image-Induced Nonlocal Means Filter. IEEE Transactions on Biomedical Engineering. 2016; 63(5): 1044-1057.
[24] Ramadan ZM. Salt-and-Pepper Noise Removal and Detail Preservation Using Convolution Kernels and Pixel Neighborhood. American Journal of Signal Processing. 2014; 4(1): 16-23.
[25] Sheik Fareed SB, Khader SS. Fast adaptive and selective mean filter for the removal of high-density salt and pepper noise. IET Image Processing. 2018; 12(8): 1378-1387.
[26] Kang B, Choi O, Kim JD. Hwang D. Noise reduction in magnetic resonance images using adaptive non-local means filtering. Electronics Letters. 2013; 49 (5): 324-326.
[27] Ramadan ZM. Using Entropy and 2-D Correlation Coefficient as Measuring Indices for Impulsive Noise Reduction Techniques. International Journal of Applied Engineering Research. 2017; 12(21): 11101-11106.

BIOGRAPHY OF AUTHORS

Zayed M. Ramadan
Dr. Ramadan earned Ph.D. and M.S. Degrees in Electrical Engineering from the University of Alabama in Huntsville, AL, USA. He also earned M.S. and B.S. degrees in Electrical Engineering from Jordan University of Science and Technology, Jordan. He is an author of numerous publications in peer-reviewed journals indexed in Scopus and ISI, a coauthor of a textbook on adaptive filtering with MATLAB published by CRC Press (Taylor and Francis Group). He has a massive teaching experience of a wide range of EE courses in various universities in USA, UAE, Jordan and KSA and received several excellence of scientific research awards. Currently, Dr. Ramadan is working in the Electrical Engineering Department at King Faisal University.